Structure is lost incrementally during the unfolding of barstar

G.S. Lakshmikanth[1], K. Sridevi[2], G. Krishnamoorthy[1] and Jayant B. Udgaonkar[2]

[1]*Department of Chemical Sciences, Tata Institute of Fundamental Research Mumbai 400005, India.* [2]*National Centre for Biological Sciences, Tata Institute of Fundamental Research, Bangalore 560065, India.*

Coincidental equilibrium unfolding transitions observed by multiple structural probes are taken to justify the modeling of protein unfolding as a two-state, N ⇌ U, cooperative process. However, for many of the large number of proteins that undergo apparently two-state equilibrium unfolding reactions, folding intermediates are detected in kinetic experiments. The small protein barstar is one such protein. Here the two-state model for equilibrium unfolding has been critically evaluated in barstar by estimating the intramolecular distance distribution by time-resolved fluorescence resonance energy transfer (TR-FRET) methods, in which fluorescence decay kinetics are analyzed by the maximum entropy method (MEM). Using a mutant form of barstar containing only Trp 53 as the fluorescence donor and a thionitrobenzoic acid moiety attached to Cys 82 as the fluorescence acceptor, the distance between the donor and acceptor has been shown to increase incrementally with increasing denaturant concentration. Although other probes, such as circular dichroism and fluorescence intensity, suggest that the labeled protein undergoes two-state equilibrium unfolding, the TR-FRET probe clearly indicates multistate equilibrium unfolding. Native protein expands progressively through a continuum of native-like forms that achieve the dimensions of a molten globule, whose heterogeneity increases with increasing denaturant concentration and which appears to be separated from the unfolded ensemble by a free energy barrier.

The two-state analyses of sigmoidal equilibrium unfolding transitions, which are seen for virtually all proteins, have been crucial in evaluating protein stabilities. The inherent presumption in such an analysis, that only two states exist at equilibrium, might appear aberrant when the complexity of the energy landscape existing between the native (N) and unfolded (U) forms, according to which folding intermediates (I) might be expected to accumulate. The discovery that many small proteins meet not only the equilibrium criteria of two-state folding[1], but also the kinetic criteria[2,3], has not only reinforced the legitimacy of two-state folding models but has also contributed to the view that folding intermediates are merely kinetic traps with no productive roles[4,5].

Time-resolved fluorescence resonance energy transfer (TR-FRET) methods have emerged as powerful tools to estimate the distance between two points (a donor and acceptor pair) in proteins, and, more important, to measure changes in this distance that accompany structural changes[6–11]. Unlike probes such as fluorescence intensity or circular dichroism (CD), which report on the average properties of all forms of a protein that are present, TR-FRET can differentiate between the N, U and I forms and yield structural information on these forms. In this method, energy transfer efficiency is estimated by collecting the decays of fluorescence intensity of the donor fluorophore in the presence or absence of an acceptor fluorophore. When such fluorescence intensity decays are analyzed by the maximum entropy method (MEM), distributions of fluorescence lifetimes are obtained[12–14], which can be used to generate a distribution of distances between the donor and acceptor.

Here, we report the use of TR-FRET coupled to MEM analysis in studying the equilibrium populations of the small 89-residue protein, barstar, in different concentrations of two chemical denaturants. In kinetic experiments, the folding, as well as unfolding, of barstar appears to be multistate with discrete intermediates populating parallel pathways[15–19]. In equilibrium experiments, the unfolding-folding reaction appears to be two-state under many different environmental conditions[20,21] and for many different engineered forms[18,22]. Nevertheless, perturbation of a specific tertiary hydrogen bond in a mutant form of barstar destabilizes the N state with respect to folding intermediates such that

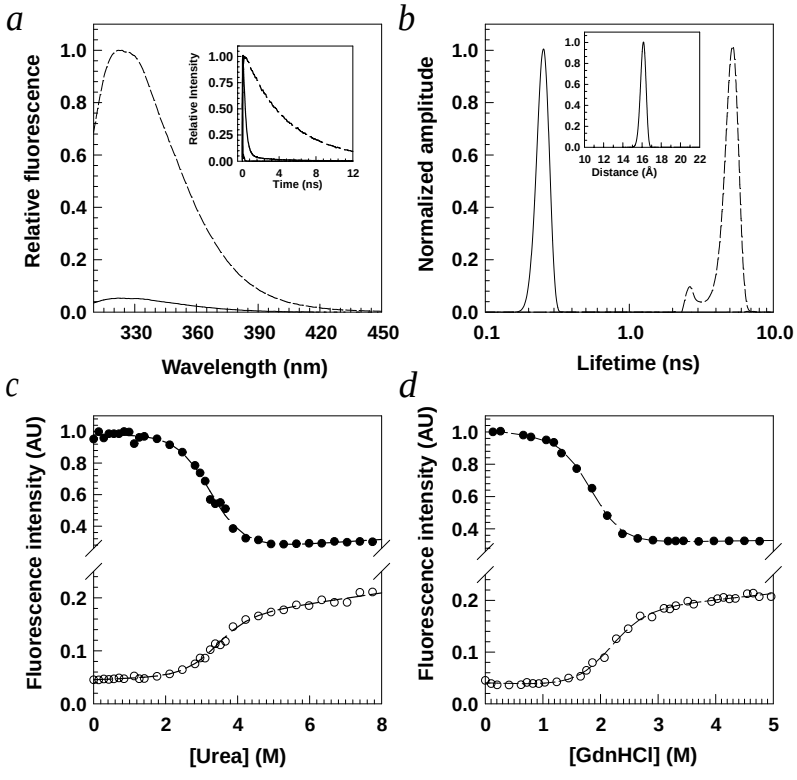

Fig. 1 FRET measurement of distance and stability. ***a***, Fluorescence spectra of the W38F/W44F/C40A mutant form of barstar. The dashed line represents unlabeled protein, and the solid line, protein labeled at Cys 82 by TNB. Inset: Fluorescence decay kinetics of unlabeled (dashed line) and labeled (solid line) proteins. ***b***, Fluorescence lifetime distributions of unlabeled (dashed line) and labeled (solid line) protein obtained by MEM analysis. Note the logarithmic scale of fluorescence lifetime. The inset shows the distance distribution plot obtained by analyzing the lifetime distribution of the labeled protein using Eq.1. The χ^2 values corresponding to the MEM distributions were 1.1 and 1.03 for labeled and unlabeled proteins, respectively. ***c***, Urea-induced equilibrium unfolding curves of labeled (open circle) and unlabeled (filled circle) proteins, monitored by fluorescence intensities at 320 nm and 360 nm, respectively. ***d***, GdnHCl-induced equilibrium unfolding curves of labeled (open circle) and unlabeled (filled circle) protein, monitored by the fluorescence intensities at 320 nm and 360 nm, respectively.

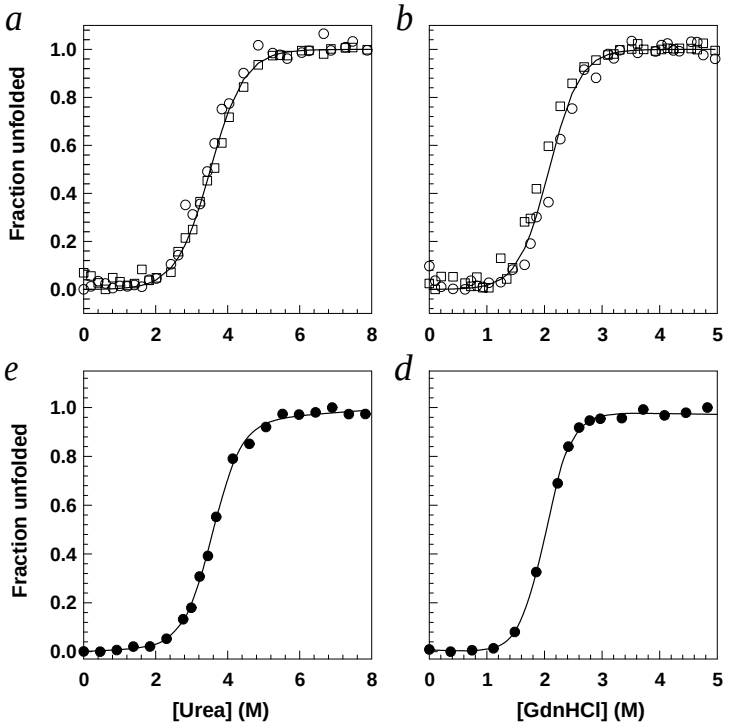

Fig. 2 Equilibrium unfolding curves. ***a***, Fraction unfolded of labeled protein calculated from measurements of the fluorescence intensity at 360 nm (open circle) and the ellipticity at 222 nm (open square) at different urea concentrations. Lines through the data represent nonlinear least-squares fits to a two-state folding mechanism, which yielded values for ΔG and C_m of 4.2 kcal mol^{-1} and 3.4 M, respectively (for labeled protein, CD- and fluorescence intensity-monitored). ***b***, Fraction of unfolded labeled protein calculated from measurements of the fluorescence intensity at 360 nm (open circle) and the ellipticity at 222 nm (open square) at different GdnHCl concentrations. Lines through the data represent nonlinear least-squares fits to a two-state folding mechanism, which yielded values for ΔG and C_m of 4.2 kcal mol^{-1} and 1.9 M, respectively (for labeled protein, CD- and fluorescence intensity-monitored). Fraction unfolded of labeled protein calculated from equilibrium unfolding transitions monitored by TR-FRET in ***c***, urea and ***d***, GdnHCl. The fraction of protein present in the U-like form was determined from TR-FRET measurements (open circle) of fluorescence lifetime distributions. The area under the lifetime distribution corresponding to U-like forms was divided by the total area under the U-like distribution at the highest denaturant concentration. The solid lines through the data represent the fraction of protein unfolded, determined by two-state analysis of the data in (*a*) and (*b*), for (*c*) and (*d*), respectively.

intermediates accumulate sufficiently to be detectable by fluorescence intensity and CD measurements[23]. This result suggests that intermediates may accumulate at equilibrium but are not discernible, even for the wild type and mutant forms of the protein that otherwise appear to undergo two-state unfolding. Here, a mutant form of barstar (W38F/W44F/C40A) containing a single Trp at position 53 and a single Cys at position 82 is used. Cys 82 was labeled using 5,5'-dithio-bis(2-nitrobenzoic acid)(DTNB). The thionitrobenzoate (TNB) group linked to Cys 82 serves as an efficient nonfluorescent acceptor of tryptophan fluorescence[22,24] and does not alter the stability or structure of barstar[22].

Distance distribution in the N state

Trp 53 is completely buried in the core of the protein and shows maximum fluorescence emission at 330 nm in the N state of the unlabeled protein. Both the emission spectra and the intensity decay kinetics show that the fluorescence of Trp 53 is quenched dramatically in the TNB-labeled protein (Fig. 1*a*). The distributions of fluorescence lifetimes of labeled and unlabeled proteins, obtained by analyzing the fluorescence decays using MEM (Fig.1*b*), show a large shift in the lifetime distribution, from ~4.97 ns to ~0.24 ns. When the TNB is attached to Cys 40 or Cys 62 in other single Cys-containing mutant forms of barstar, large but different shifts in the lifetimes are also seen (data not shown), indicating that quenching is distance-dependent and, therefore, most likely due to FRET. The quenching is found to be independent of the protein concentration used, which indicates the absence of intermolecular energy transfer (data not shown).

That quenching is due to FRET is supported by the recovery of the correct intramolecular distance from FRET analysis. The lifetime distribution can be translated into a distribution of distance, R, between donor and acceptor using Forster's relation:

$$E = (1 + R^6 R_0^{-6})^{-1} = 1 - \tau_{da}\tau_d^{-1} \quad (1)$$

$$R_0 = (8.8 \times 10^{23}\, \kappa^2\, n^{-4}\, Q_D\, J)^{1/6}\ (\text{Å}) \quad (2)$$

where R_0 is the Forster's distance, J is the overlap integral, Q_D is the quantum yield of unlabeled protein fluorescence, n is the refractive index of the medium and κ^2 is the orientation factor[25,26]. J is determined as the overlap between the fluorescence emission spectrum of unlabeled N and the absorption spectrum of labeled N (data not shown), and Q_D is determined to be 0.27. The value to be used for κ^2 depends the orientation of Trp 53 and the TNB moeity with respect to each other. The distance distribution (Fig. 1*b*, inset) is obtained by mapping the lifetime distribution (τ_{da}) of the labeled protein with the peak value of the lifetime distribution obtained from the unlabeled (τ_d) protein. The narrow width associated with the lifetime distribution (Fig. 1*b*) suggests a fast averaging of all possible orientations rather than a single relative orientation. This is not surprising because even though the TNB[22] attached to Cys 82, as well as unlabelled Trp 53 (ref. 27), is buried, the hydrophobic core in barstar is known to be highly dynamic, with many side chains appearing to undergo fast motions in the ns or faster time scale[28].

Obtaining a range of possible values for κ^2 from measurements of the decays of fluorescence anisotropies of the donor and acceptor probes is possible[8,29,30]. For the donor Trp 53, no fast local motion has been reported[6], but the time-resolution of the previous and the present measurements precludes the measurement of any decay in anisotropy that would be complete in less than 30 ps. Indeed, if the initial anisotropy, r_0, of Trp 53 (ref. 6) in barstar is determined by extrapolation of the observed anisotropy decay kinetics to t = 0, its value is 0.2. This value is only half of the value of r_0 (0.4) determined by sub-ps measurements for Trp either free in solution[31] or in other proteins[32], suggesting that half of the initial anisotropy of Trp 53 decays in less than 30 ps. For acceptor measurements, since TNB is not fluorescent, Cys 82 was labeled alternatively with other fluorescent probes, 1,5-IAEDANS and Dansyl aziridine, and the anisotropy decay kinetics of these probes were measured. In either case, two rotational correlation times, 0.3 ns and 4 ns, are observed. The fast decay in anisotropy occurs at about the same rate as that observed for the free probes

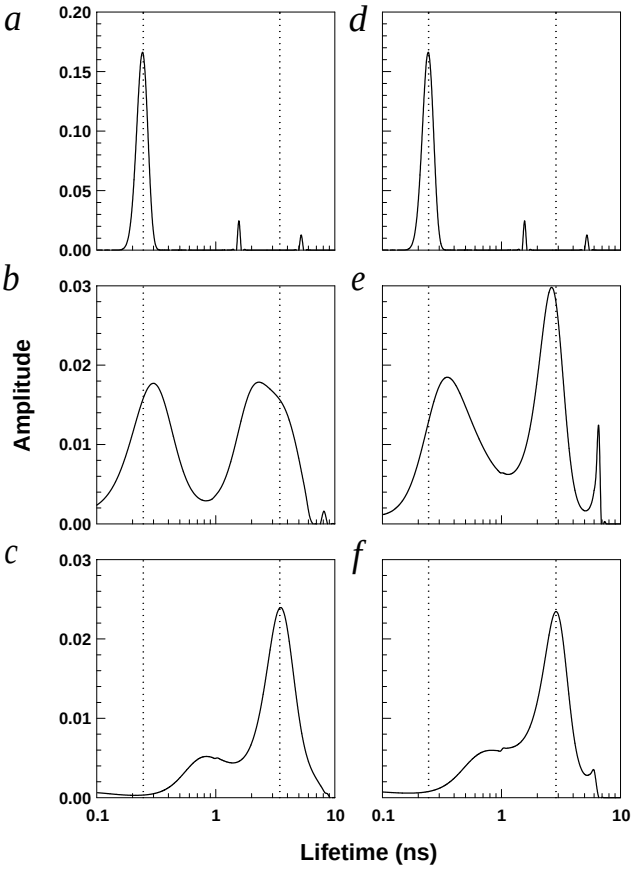

Fig. 3 Fluorescence lifetime distributions of labeled protein. Fluorescence lifetime distributions were determined in ***a***, 0 M Urea; ***b***, 3.7 M Urea; ***c***, 8.0 M Urea; ***d***, 0 M GdnHCl; ***e***, 2.2 M GdnHCl and ***f***, 6 M GdnHCl. The dotted lines indicate the positions of the peaks of the distributions of lifetimes for the N state and U form. The χ^2 values for these distributions were 1.1, 1.14, 1.12, 1.10, 1.15 and 1.03 for (*a*–*f*), respectively. The positions, widths and relative areas under the distributions did not vary for longer times of incubation, indicating that the measurements were indeed made under equilibrium conditions.

in solution. Further, the combined amplitude of the fast decay process with unresolved fast motions is 70%.

These measurements indicate that the value for κ^2 is in the range 0.25–2.3 for either fluorescent acceptor[29,33], but this range would be narrower if the multiple transition dipoles for both absorption and emission[34], which are known to exist for many fluorophores including indole[33] and DANS derivatives[34], could also be taken into account. The range is expected to be even narrower when TNB is the acceptor, because TNB, significantly smaller than AEDANS or DANS, is expected to have considerably less restricted motion. Because DANS is linked to Cys 82 by a shorter arm than is AEDANS, the observation that the anisotropy decay kinetics are the same for both probes suggests that the motional freedom of a probe attached to this site is determined more by its size than the length of its linker arm. In view of these observations, which indicate that donor and acceptor are indeed oriented randomly with respect to each other, proceeding with the assumption that $\kappa^2 = 2/3$ (refs 29,34) appears reasonable. Estimates of distances made with this assumption are found to match estimates obtained using other methods[35] for other proteins.

R_0 is calculated to be 26.6 Å for the N state of barstar. Hence, R between Trp 53 and Cys 82-TNB is determined to be 16.2 ± 0.2 Å (Fig. 1*b*). Given the size of the TNB moiety, this agrees well with the distance of 15.5 Å calculated (between the indole ring of Trp 53 and the S atom of the Cys 82) from the NMR structure[27]. In this context, even if Cys82-TNB is oriented towards Trp 53, it can have a conical wobbling motion about the axis connecting Cys 82 and Trp 53, resulting in the observed fast 70% depolarization of fluorescence. Similarly, the TR-FRET-determined distances of 18.1 Å and 13.8 Å between Trp 53 and Cys 40-TNB and Cys 62-TNB, respectively, in two other single Cys-containing mutant proteins agree well with the NMR structure-determined distances of 14.6 Å and 12.6 Å, respectively (data not shown). This agreement constitutes the best test[8] for the validity of the assumption made here and elsewhere[35], that $\kappa^2 = 2/3$.

The quenching caused by energy transfer is released when the protein is unfolded by urea or guanidine hydrochloride (GdnHCl) (Fig.1*c*,*d*). Unlike the fluorescence intensity of the unlabeled protein, which decreases upon unfolding because Trp 53 becomes solvent-exposed, that of the labeled protein increases consequent to Trp 53 and Cys 82-TNB becoming further separated.

Distance distribution in the unfolded form

As in the case of the native protein (Fig.1*b*), the distribution of lifetimes in the unfolded protein is shifted to shorter values upon labeling, because energy transfer also occurs in U (Fig. 1*c*, *d*). Unlike the large shift upon labeling observed for N, the shift observed for U is small: the mean fluorescence lifetime of U in 6 M GdnHCl is shifted from 2.50 to 2.22 ns upon labeling (data not shown). The width associated with the lifetime distribution in U is broader than that observed for N, for the labeled as well as unlabeled proteins, implying greater heterogeneity in the population of unfolded forms. Indeed, this is expected for a random coil U. This heterogeneity causes uncertainty in the estimation of the distance distribution in U; the broad distribution of lifetimes present in unlabeled U precludes the use of a single value of τ_d in generating a distance distribution.

Two-state unfolding detected by steady-state probes

The steady state spectroscopic probes (Figs 1*c*,*d* and 2*a*,*b*) make several important points. First of all, two-state analysis of the sigmoidal equilibrium unfolding curves determined by fluorescence intensity measurements yield the same value for ΔG, 4.1 ± 0.5 kcal mol^{-1}, for both urea and GdnHCl-induced unfolding of the unlabeled protein. This value of ΔG for the unlabeled protein is similar to the value reported earlier for ΔG of the wild type protein, indicating that replacement of Trp 38 and Trp 44 by Phe, and Cys 40 by Ala, does not alter the stability. In addition, the sigmoidal equilibrium unfolding transitions for the labeled protein are completely coincident when measured by CD and fluorescence, which indicates that the labeled proteins undergo two-state unfolding. Because the value for ΔG, 4.2 ± 0.5 kcal mol^{-1}, for the labeled protein is nearly identical to the value for the unlabeled protein, the chemical label only marginally increases the stability of the protein. Lastly, labeling does not alter the secondary structure of the protein, because the labeled and unlabeled proteins behave identically with respect to ellipticity measurements at 222 nm.

Partially unfolded forms during equilibrium unfolding

The distributions of lifetimes, determined by TR-FRET in the folding transition zones of the equilibrium unfolding curves of the labeled protein, are of particular interest. The distribution obtained either in 2.2 M GdnHCl or 3.7 M urea, which are close to the midpoints of the GdnHCl-induced and urea-induced transitions, do not correspond to a linear combination of the

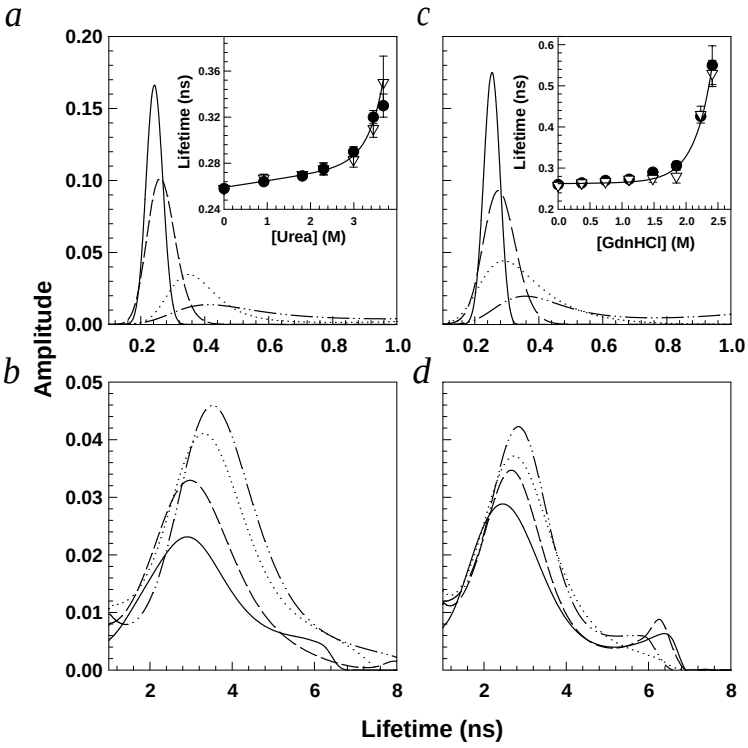

Fig. 4 Fluorescence lifetime distributions of N-like and U-like forms. ***a***, Distribution in various concentrations of urea for the N-like form. The solid, dashed, dotted and dash-dotted lines represent distributions in 0 M urea, 1.8 M urea, 3.2 M urea and 3.6 M urea, respectively. ***b***, The U-like form in various concentrations of urea: 3.7 M urea (solid), 4.1 M urea (dashed), 6 M urea (dotted) and 8 M urea (dashed-dotted). ***c***, The N-like form in various concentration of GdnHcl. The solid, dashed, dotted and dash-dotted lines represent distributions 0 M GdnHCl, 1.1 M GdnHCl, 1.9 M GdnHCl and 2.4 M GdnHCl, respectively. ***d***, Distribution of the U-like form in various concentrations of GdnHCl: 2.4 M GdnHCl (solid), 2.6 M GdnHCl (dashed), 4.1 M GdnHCl (dotted) and 6 M GdnHCl (dashed-dotted). Insets in (*a*,*c*): Plots of the peak position of N-like forms from the MEM distribution (filled circle) and the fluorescence lifetime obtained from discrete analysis of decay kinetics (open, inverted triangle) *versus* denaturant concentration. The errors in both the MEM peak positions and discrete lifetimes, as determined from multiple experiments, are in the range of 5–10%. The lines are drawn by inspection. The χ^2 values for both the MEM distribution analysis and the discrete analysis were in the range of 1.0–1.2.

distributions obtained in N and U (Fig. 3). Furthermore, the widths of the distributions in the middle of the transitions are broader when compared to those of N and U.

Lifetime distributions obtained in various concentrations of urea (Fig. 4*a*,*b*) and GdnHCl (Fig. 4*c*,*d*) can be classified as belonging either to native-like (N-like) forms, with lifetimes between 0.1 and 1 ns, or to unfolded-like (U-like) forms, with lifetimes >1.0 ns. The salient features of the data are (i) in the N-like forms (Fig. 4*a*, *c*), both in urea and GdnHCl, there is a gradual shift of the peak of the distributions towards longer lifetimes with increasing denaturant concentration; (ii) there is a simultaneous increase in the width of the distribution of lifetimes, suggesting that the N-like forms transform gradually to a population of enhanced heterogeneity before transforming to U-like forms; (iii) the peak position but not the width of the distribution of lifetimes in U-like forms shifts with increasing denaturant concentration; and (iv) with increasing denaturant concentration, the area under the distributions of U-like forms, which reflects the number of U-like molecules, increases at the expense of a decrease in area of the distribution of N-like forms, which reflects the number of N-like molecules.

A trivial explanation for the increase in lifetimes between 0.1 and 1 ns would be that it represents a change in the N state with changes in denaturant concentration. This explanation is unlikely to be correct for the following reasons: (i) no such increase is observed for unlabeled protein (data not shown), and (ii) for other mutant proteins, in which the TNB is attached to either Cys 40 or Cys 62, the fractional increases in lifetime are different from that seen with the TNB attached to Cys 82, whereas a general solvent effect would have resulted in similar fractional increases (data not shown).

Incremental unfolding

N undergoes unfolding through a continuum of N-like forms, whose fluorescence lifetimes increase progressively with denaturant concentration (Fig. 4). Ensemble-averaged spectroscopic signals, such as fluorescence intensity and ellipticity, do not distinguish between these N-like forms (Figs 1, 2). However, the TR-FRET technique coupled with MEM analysis enables the visualization of subtle changes in structure within the population of N-like forms, with increasing denaturant concentration.

Given the small observed shifts in lifetime distributions, even though they were repeatedly seen in measurements on a large number of samples, confirming the value of the peak of the lifetime distribution obtained by MEM analysis by another method of analysis was important. Each fluorescence decay curve was also analyzed as a sum of discrete lifetimes; the lifetime of the N-like form obtained by discrete lifetime analysis consistently matched the peak of the lifetime distribution obtained by MEM analysis (Fig. 4*a*,*c*, inset).When discrete lifetime analysis was also performed by forcing the lifetime of a N-like form to be that of the N state, statistically unsatisfactory fits were obtained, both by the criteria of χ^2 values and by the observation of nonrandom distributions of residuals (data not shown). This confirmed that each N-like form has a different lifetime that is shifted from that of the N state.

The observed gradual increase in the lifetime of labeled protein, with increase in denaturant concentration, can also be modeled as due to very rapid exchange between the N state and a single intermediate instead of continuously changing N-like forms. This is, however, unlikely because (i) fast exchange would demand that the rate of exchange be faster than 10^{10} s^{-1}, the fastest rate of fluorescence decay, whereas conformational changes in proteins[36] are found typically to be slower than 10^9 s^{-1}, and (ii) the increase in the width of the lifetime distribution with increase in the denaturant concentration cannot be explained by the fast exchange model.

Although intrachain diffusion and fast conformational fluctuations occurring during the excited state lifetime[34,37,38] could complicate the interpretation of TR-FRET, this is unlikely because any increase in fast conformational fluctuations with increase in the concentration of denaturants will only enhance the FRET; in contrast, the extent of FRET is seen to decrease. Also, diffusion and fluctuations, if present, should be temperature-dependent, but the widths of the distributions seen here at 25 °C are found to be nearly identical to those seen at 10 °C (data not shown).

The distributions of lifetimes (Fig. 4) for N-like forms in denaturant concentrations extending to the midpoint of the unfolding transition were transformed to distributions of the distance, R, between Trp 53 and Cys 82-TNB, using Eq. 1. To determine R for the N-like forms, first determining R_0 for each of these forms is

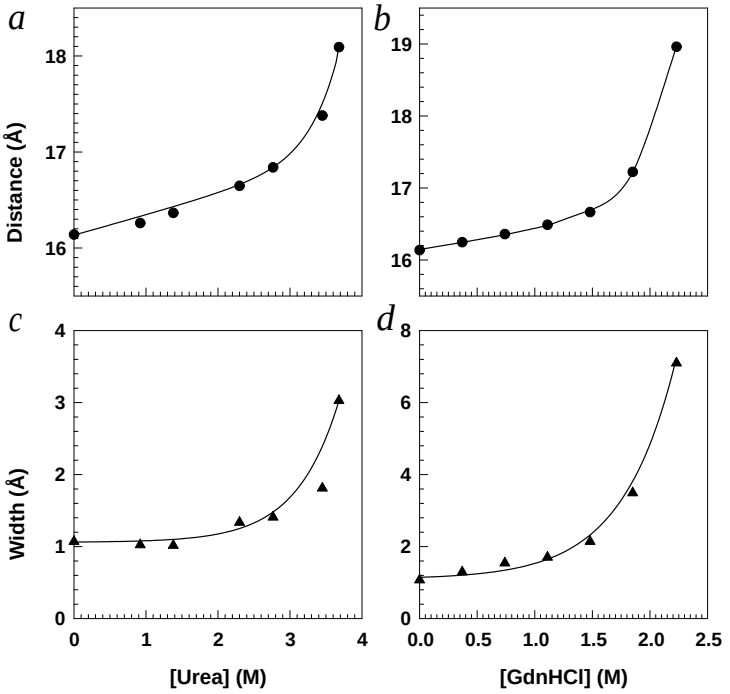

Fig. 5 Denaturant-dependence of the separation and width of the distribution of distances between Trp 53 and Cys 82-TNB in N-like forms. ***a***,***b***, Distance between the donor and acceptor in different concentrations of urea and GdnHCl, respectively. ***c***,***d***, Width of the distribution of distance between donor and acceptor in different concentrations of urea and GdnHCl, respectively. The distances were calculated, using Eq. 1, from the peaks of the fluorescence lifetime distributions obtained for the labeled and unlabeled protein (Fig. 4) at various concentrations of denaturant. The distance estimate did not change significantly when the mean value of the lifetime distribution was used instead of the peak value. Lifetime distributions were transformed into distance distributions as described, and the widths were calculated as the full widths at half-maximum after fitting the amplitude distributions as Gaussian distributions. The errors in the measurements of widths are in the range of 10%. The lines are drawn by inspection.

necessary. This requires determination of Q_D and J[25,26] in each denaturant concentration. Although fluorescence spectra were measured at all denaturant concentrations, those in the transition zone of unfolding represent the weighted sums of the spectra of N-like and U-like forms, because both of these forms are present. Therefore, the value of Q_D for the N-like forms at each denaturant concentration cannot be determined directly from the fluorescence emission spectrum. Unlike fluorescence intensity measurements, time-resolved measurements of fluorescence decay allow the N-like and U-like components to be distinguished in the unlabeled protein. For the relevant concentrations of denaturant, the lifetime distribution of the N-like forms (of the unlabeled proteins) is nearly identical to that of the N state: the peak value (τ_d) varies only from 4.9 to 5 ns, and the width varies from 1 to 1.5 ns (data not shown). Thus, a single value for the lifetime τ_d, identical to that determined for the N state, can be used for all N-like forms. Hence, the value of Q_D for all N-like forms can be taken to be the same as that of the N state, 0.27. This also allows the fluorescence emission spectrum of the N state to represent those of all N-like forms. The absorbance spectra of TNB in the labeled protein were measured and show a red-shift of only ~3 nm over a range of denaturant concentrations extending to the mid-point of the unfolding transition (data not shown); thus, the value of J does not vary significantly from the N state to the N-like forms. Values for R_0 of 26.6, 26.6, 26.5 and 26.4 Å were obtained in 0, 0.5, 1.0 and 2.0 M GdnHCl, respectively. Hence, an average value of 26.5 Å for R_0 was used for the N-like forms.

The distance increases gradually with urea (Fig. 5*a*) or GdnHCl (Fig. 5*c*) concentration, respectively. This increase in mean distance is seen even when the decay curves are analyzed by a discrete lifetime model instead of MEM. The change in a structural parameter, such as the distance between donor and acceptor, implies that the N-like forms are structurally distinct from the N state. The width associated with each distribution of distance also increases gradually with increasing denaturant concentration, showing that the heterogeneity of the N-like population is increasing (Fig. 5*b*,*d*). The progressive increase in width of the distributions of the N-like forms cannot be due to a progressive decrease in the fast averaging of orientations of the donor with respect to the acceptor, because the dynamics are expected to be faster in N-like forms than in the N state. The increase in width must instead represent an increase in the distribution of distance between the donor and acceptor.

Unfolding through a continuum of forms

After MEM analysis, the fraction of molecules present as U at each denaturant concentration can be determined by dividing the area under the U-like distribution by the area under the U distribution at the highest concentration of denaturant used (Fig. 2*c*,*d*). The fraction of molecules determined to be U by two-state analysis (Fig. 2*a*,*b*) is overlaid in Fig. 2*c*,*d*. There is complete coincidence between the values for fraction unfolded determined by TR-FRET and by either fluorescence intensity or ellipticity measurements. This observation implies that a free energy barrier exists between the N-like and U-like forms and that molecules crossover from the N-like forms to the U-like forms by a first order process. At present, whether the transitions between the N-like forms are higher order transitions, with no free energy barriers separating them, is not known[39]. If true, this would suggest that noncooperative structural changes with little energy cost precede, and may be a prerequisite to, the major cooperative unfolding transition. Spectroscopic probes such as fluorescence intensity or ellipticity cannot distinguish between N and N-like forms. As a result, the equilibrium unfolding transition appears to be two-state. TR-FRET measurements show clearly, however, that the distance between Trp 53 and Cys 82-TNB increases in the N-like forms with an increase in denaturant concentration. Similar results are obtained with other TNB labeled mutant proteins in which the single Cys is at position 40 or 62 along the sequence (data not shown).

The distance between Trp 53 and Cys 82-TNB in the N-like forms increases by about 2 Å upon increasing the concentration of either denaturant to that corresponding to the mid-point, C_m, of the equilibrium unfolding transition (Fig. 5). Assuming that the radius of the protein also increases by the same proportion, this corresponds to an ~45% increase in the overall volume of the protein. This significant change in volume corresponds to the decrease in volume, determined by measurement of global rotational correlation times, that occurs when the late intermediate I_N transforms to N on the major folding pathway[19] and also to the expansion that a native protein typically undergoes when it transforms to a molten globule[40]. The N-like forms appear to resemble molten globule intermediates not only in size but also in being truly molten: they expand gradually with an increase in denaturant concentration. The distance distribution clearly indi-

cates that barstar unfolds through a continuum of native-like forms with progressively changing structure rather than by a strict two-state mechanism. To date, such gradual loss or formation of structure has only been inferred from Langevin simulation of off-lattice models for the formation of secondary structure in hairpin loops[41].

A central question concerning proteins with apparent two-state folding, according to both kinetic and thermodynamic criteria, is whether they are genuine two-state folders or whether intermediates are not detected in kinetic and equilibrium experiments because they are too unstable. For the archetypal two-state folding protein, chymotrypsin inhibitor-2, no intermediates were detected in kinetic experiments[2], in native-state hydrogen exchange experiments (see ref. 42 for review) or in equilibrium measurements of FRET on single molecules in solution[9]. Several other apparently genuine two-state folders, however, display native baselines with steep denaturant dependences in equilibrium unfolding experiments[43,44], which could be suggestive of intermediates. For the characterization of equilibrium unfolding intermediates, ensemble measurements of TR-FRET coupled with MEM analysis appear to be an attractive alternative to single molecule measurements of FRET.

Methods

Purification and labeling of the mutant protein W38F/W44F/C40A. The mutant protein was prepared and labeled as described[22].

Fluorescence and CD measurements. Fluorescence measurements were carried out using a Spex Fluorolog FL1T11 fluorimeter, with the excitation wavelength set at 295 nm. CD measurements were made on a Jasco 720 spectropolarimeter as described[20]. All measurements were done at 25 °C. Concentrations of the protein used were 5–40 μM in 50 mM Tris buffer and 0.5 mM EDTA, pH 8. In the range of protein concentrations used, the absence of protein aggregation was confirmed by dynamic light scattering studies. Equilibration with denaturants was carried out for ~60 min prior to any spectroscopic measurement. The refractive index, n, of each denaturant solution was measured using an Abbe-type refractometer.

Analysis of equilibrium unfolding transitions. Measurements of fluorescence intensity or CD in different denaturant concentrations were analyzed according to a two-state, $N \rightleftharpoons U$, mechanism[20].

Time-resolved fluorescence measurements. Time resolved anisotropy experiments were carried out as described[6]. Time-resolved fluorescence intensity decay curves were collected up to 99.9% of completion with a peak count of at least 20,000, as described[45]. These conditions of data collection ensured robustness of the parameters recovered by MEM analysis[14,40].

MEM Analysis. MEM analysis is independent of any physical model or mathematical equation describing the distribution of lifetimes, which distinguishes it from other methods[46–49] of analyzing fluorescence decays. MEM analysis of the fluorescence decay curves was carried out as described [14,50] to obtain distributions of fluorescence lifetimes in a model-independent manner. The robustness of the lifetime distributions (including peak positions and widths of distributions) obtained by MEM analysis was checked exhaustively by (i) analyses of data collected several times on the same sample and (ii) collecting data on several samples under the same sample conditions. Values of χ^2 were in the range of 1.0 to 1.2 for all the MEM analyses. Peak values of MEM distributions agreed with those obtained from discrete lifetime analyses to within ~5%. Errors in the peak values and widths of lifetime distributions obtained by MEM were 5–10% and 10–15%, respectively. For example, the change of 2 Å in the mean distance (Fig. 5) corresponds to a change in the peak value from 0.24 to 0.4 ns. The level of accuracy in these values are about 0.23–0.25 and 0.38–0.42, respectively. This level of accuracy was also obtained in discrete life time analyses. The error in the estimation of distance is therefore ±0.1 Å.

Acknowledgments

We thank N. Periasamy for the MEM software and advice on its use; A.S.R. Koti for discussion and help regarding MEM analysis; and M.K. Mathew, S. Mayor and B. Rami for critical reading of the manuscript. This work was funded by the Tata Institute of Fundamental Research and by the Wellcome Trust. J.B.U. is the recipient of a Swarnajayanti Fellowship from the Government of India.

Correspondence should be addressed to G.K. *email: gk@tifr.res.in* and J.B.U. *email: jayant@ncbs.res.in*

Received 27 December, 2000; accepted 13 July, 2001.

1. Tanford, C. *Adv. Protein Chem.* **21**, 1–95 (1970).
2. Jackson, S.E. & Fersht, A.R. *Biochemistry* **30**, 10428–10435 (1991).
3. Plaxco, K.W., Simons, K.T., Ruczinski, I. & Baker, D. *Biochemistry* **39**,11177–11183 (2000).
4. Dobson, C.M., Sali, A. & Karplus, M. *Angew. Chem. Int. Ed.* **37**, 868–893 (1998).
5. Chan, H.S. & Dill, K.A. *Proteins* **30**, 2–33 (1998).
6. Swaminathan, R., Nath, U., Udgaonkar, J.B., Periasamy, N. & Krishnamoorthy, G. *Biochemistry* **35**, 9150–9157 (1996a).
7. Tcherkasskaya, O., Knutson, J.R., Bowley, S.A., Frank, M.K. & Gronenborn, A.M. *Biochemistry* **39**, 11216–11226 (2000).
8. Lillo, M.P., Beechem, J.M., Szpikowska, B.K., Sherman, M.A. & Mas, M.T. *Biochemistry* **36**, 11261–11272 (1997).
9. Deniz, A.A *et al. Proc. Natl. Acad. Sci. USA* **97**, 5179–5184 (2000).
10. Shih, W.M., Gryczynski, Z., Lakowicz, J.R. & Spudich, J.A. *Cell* **102**, 683–694 (2000).
11. Talaga, D.S. *et al. Proc. Natl. Acad. Sci. USA* **97**, 13021–13026 (2000).
12. Skilling, J. & Bryan, R.K. *Mon. Not. R. Astr. Soc.* **211**, 111–124 (1984).
13. Brochon, J.C. *Methods Enzymol.* **240**, 262–311 (1994).
14. Swaminathan, R. & Periasamy, N. *Proc. Indian Acad. Sci. Chem. Sci.* **108,** 39–49 (1996).
15. Agashe, V.R., Shastry, M.C., & Udgaonkar, J.B. *Nature* **377**, 754–757 (1995).
16. Shastry, M.C. & Udgaonkar, J.B. *J. Mol. Biol.* **247**, 1013–1027 (1995).
17. Zaidi, F.N., Nath, U. & Udgaonkar, J.B. *Nature Struct. Biol.* **4**, 1016–1024 (1997).
18. Nolting, B. *et al. Proc. Natl. Acad. Sci. USA* **94**, 826–830 (1997).
19. Sridevi, K., Juneja, J., Bhuyan, A.K., Krishnamoorthy, G. & Udgaonkar, J.B. *J. Mol. Biol.* **302**, 479–495 (2000).
20. Agashe, V.R. & Udgaonkar, J.B. *Biochemistry* **34**, 3286–3299 (1995).
21. Khurana R., Hate A.T., Nath, U. & Udgaonkar, J.B. *Protein Sci.* **4**, 1133–1144 (1995).
22. Ramachandran, S. & Udgaonkar, J.B. *Biochemistry* ***35***, 8776–8785 (1996).
23. Nath, U. & Udgaonkar, J.B. *Biochemistry* **34**, 1702–1713 (1995).
24. Wu, P. & Brand, L. *Biochemistry* **33,** 10457–10462 (1994).
25. Cantor, C.R. & Schimmel, P.R. In *Biophysical chemistry* 451–454 (W. H. Freeman & Co., New York; 1980).
26. Lakowicz, J.R. In *Principles of fluorescence spectroscopy* 2nd edn 371–376 (Plenum Press, New York; 1999).
27. Lubienski, M.J., Bycroft, M., Freund, S.M. & Fersht, A.R. *Biochemistry* **33**, 8866–8877 (1994).
28. Wong, K.-B. & Daggett, V. *Biochemistry* **37**, 11182–11192 (1998).
29. Dale, R.E., Eisinger, J. & Blumberg, W.E. *Biophys. J.* **26**, 161–194 (1979).
30. Navon, A., Ittah, V., Landsman, P. Scheraga, H.A. & Haas, E. *Biochemistry* **40**, 105–118 (2001).
31. Ruggiero, A.J., Todd, D.C. & Flemming, G.R. *J. Am. Chem. Soc.* **112**, 1003–1014 (1990).
32. Hansen, J.E., Rosenthal, S.J. & Fleming, G.R. *J. Phys. Chem.* **96**, 3034–3040 (1992).
33. Lakowicz, J.R. *et al. Biochemistry* **27**, 9149–9160 (1988).
34. Haas, E., Katchalski-Katzir, E. & Steinberg, I.Z. *Biochemistry* **17**, 5064–5070 (1978).
35. Dos Remedios, C.G. & Moens, P.D.J. *J. Struct. Biol.* **115**, 175–185 (1995).
36. Ishima, R. & Torchia, D.A. *Nature Struct. Biol.*, **7**, 740–743 (2000).
37. Beechem J.M. & Haas, E. *Biophys J.* **55**, 1225–1236 (1989).
38. Eis, P.S. & Lakowicz, J.R. *Biochemistry* **32**, 7981–7993 (1993).
39. Dill, K.A. & Shortle, D. *Annu. Rev. Biochem.* **60**, 795–825 (1991).
40. Ptitsyn, O.B. In *Protein Folding* (ed. Creighton, T.E.) 243–300 (W.H. Freeman & Co., New York; 1992).
41. Klimov, D.K. & Thirumalai, D. *Proc. Natl. Acad. Sci. USA*, **97**, 2544–2549 (2000).
42. Englander, S.W. *Annu. Rev. Biophys. Biomol. Struct.* **29**, 213–238 (2000).
43. Smith, C.K. *et al. Protein Sci.* **5**, 2009–2019 (1996).
44. Plaxco K.W. *et al. Biochemistry* **37**, 2529–2537 (1998).
45. Lakshmikanth, G.S. & Krishnamoorthy, G. *Biophys. J.* **77**, 1100–1106 (1999).
46. Alcala, J.R., Gratton, E. & Prendergast, F.G. *Biophys. J.* **51,** 597–604 (1987).
47. Gryczynski, I.M. Eftink & Lakowicz, J.R. *Biochim. Biophys. Acta.* **954,** 244–252 (1988).
48. Ittah, V. & Haas, E. *Biochemistry* **34**, 4493–4506 (1995).
49. Bismuto, E., Sirnagelo, I. & Irace, G. *Arch. Biochem. Biophys.* **291**, 38–42 (1991).
50. Swaminathan, R., Krishnamoorthy, G. & Periasamy, N. *Biophys. J.* **67,** 2013–2023 (1994).